ACS APPLIED POLYMER MATERIALS

pubs.acs.org/acsapm Article

Oligomeric Curing Activators Enable Conventional Sulfur-Vulcanized Rubbers to Self-Heal

Alan M. Wemyss, Arkadios Marathianos, Ellen L. Heeley, James Ekeocha, Yoshihiro Morishita, Raffaele di Ronza, M. Mar Bernal, David M. Haddleton, and Chaoying Wan*

Cite This: https://doi.org/10.1021/acsapm.2c01398 Read Online

ACCESS | Metrics & More | Article Recommendations | Supporting Information

ABSTRACT: When introducing self-healing properties to elastomers, it is often difficult to balance their ability to recover properties after damage with a good mechanical strength prior to damage. We demonstrate that by replacing the activator system used in conventional accelerated vulcanization (CV) chemistry, from the traditional zinc oxide (ZnO) and stearic acid to a complex formed between ω-propenyl functional oligomers of poly(zinc methacrylate) (pZnMA/ZnO), the self-healing properties of vulcanized natural rubbers are enhanced while maintaining good tensile strengths. The pZnMA oligomers, as synthesized by catalytic chain transfer polymerization (CCTP), act as an activator for the sulfur curing system, while also forming an ionic network in the rubber. The addition of 20 phr of pZnMA/ZnO to a CV system resulted in a cured natural rubber with a tensile strength of 7.47 ± 0.64 MPa, which recovered 86.7% after self-healing at 80 °C for 2 h. Further addition of 40 phr of carbon black N234 unexpectedly enhanced the self-healing efficiency of these vulcanized rubbers to 92.2% under the same conditions and also improved the self-healing at room temperature. Finally, dynamic mechanical thermal analysis indicated that the natural rubber formulations containing pZnMA/ZnO showed improved wet traction but with higher rolling resistance to a standard formulation. These results point to an interesting direction for further research into the performance of self-healing composites in vehicle tire applications.

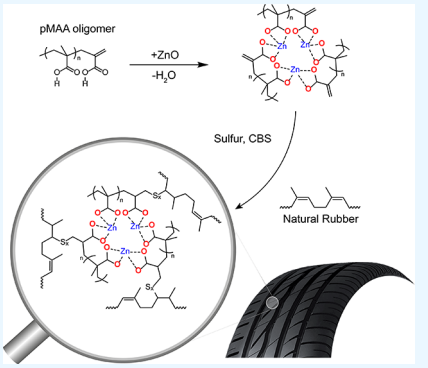

KEYWORDS: *vulcanization, rubber, curing agent, self-healing, tire tread materials*

INTRODUCTION

Vulcanized commercial elastomers are a key component of transport tires due to their high toughness and durability. There is a huge demand for these products, with around 3 billion tires being manufactured worldwide in 2019.[1] However, while these elastomers provide excellent properties, tires are multilayer thermoset networks that are extremely difficult to reprocess and recycle—a societal problem of increasing concern. While ∼80% of waste tire rubbers are reclaimed by mechanical grinding or pyrolysis processes, a large volume still ends up being incinerated or dumped into landfill each year.[2,3] A feasible and promising alternative approach to reprocessing is extending a tire's service life through the incorporation of self-healing mechanisms.[3] Not only does this reduce the generation of waste tires, but with each tire requiring in the region of nine gallons of oil to make, extending their service life would significantly reduce global oil usage.[4]

Intrinsically self-healing thermoset elastomers are created by substituting the permanent bonds that would usually cross-link these materials with nonpermanent or dynamic bonds.[5−7] Cross-linkers containing dynamic covalent bonds, such as Diels−Alder adducts,[8,9] disulfides,[10,11] and boronic esters,[12,13] have been grafted to commercial elastomers to facilitate self-healing, most commonly by either oxirane ring-opening reactions of an epoxidized rubber or by thiol−ene grafting to dienic elastomers. Peroxide curing diene rubbers with monomers containing a carbon−carbon double bond, such as maleic anhydride and methacrylic acid, and zinc oxide have also been shown to give good self-healing efficiencies in these materials due to the formation of an ionic network.[14−16] However, in these latter systems, shorter curing times and/or lower curing temperatures are typically used to suppress the number of permanent covalent bonds that form during curing, which can result in a lowering of the tensile properties of these materials.

Recently, several publications have emerged that use modified sulfur cure packages to produce self-healing materials. This is an interesting approach, as these compounds could be produced at scale with little or no modification to existing manufacturing facilities. For example, the addition of $CuCl_2$ to a semiefficient vulcanization system (semi-EV) catalyzes

Received: August 16, 2022
Accepted: August 30, 2022

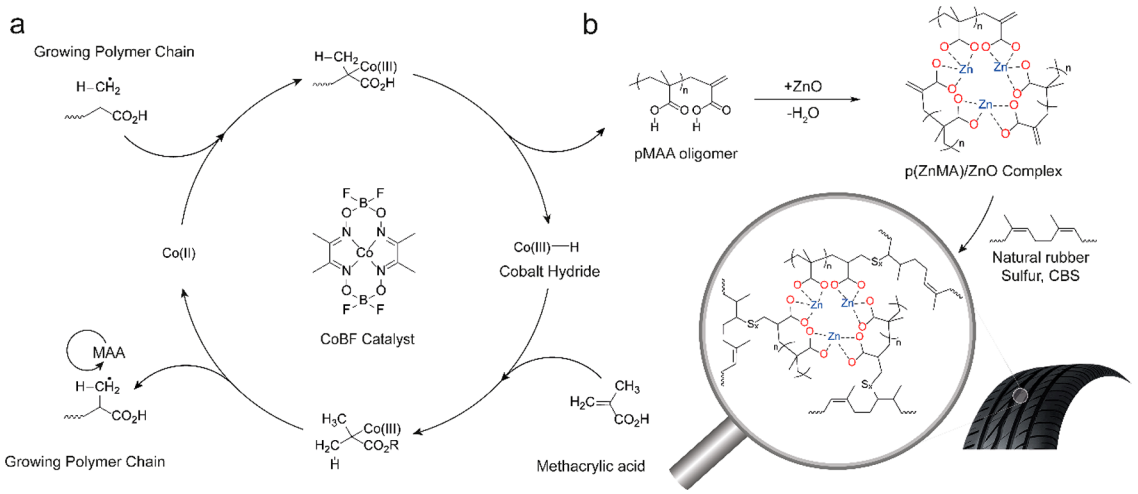

Figure 1. (a) Catalytic cycle for the CCTP synthesis of pMAA. (b) Illustration of the ionic network formed when using pZnMA/ZnO complex as curing activator for NR vulcanization.

exchange reactions between the disulfide and polysulfide bonds in the network.[17] The rubber chain mobility allowed by this process meant that these compounds were able to recover up to 72% of their original tensile strength of 3.2 MPa after self-healing for 12 h at 110 °C. Transalkylation of C−S bonds has been induced in a conventional vulcanized (CV) rubber network with the addition of sulfonium compounds.[18] In this case, samples recovered 62% of their original tensile strength of 5.8 MPa after just 2 min of self-healing at 165 °C. Interestingly, longer time frames at this temperature resulted in a decrease in their apparent self-healing efficiency due to the thermal aging of these materials. Vulcanized rubber compounds with self-healing ability have also been produced without extrinsic catalysts, but instead by lowering the amount of sulfur that is added as well as their degree of curing.[19,20] While these have shown good self-healing efficiencies at temperatures as low as 80 °C, these modifications also significantly reduce the mechanical properties of these materials.

In this work, we investigate an alternative approach to enhancing the self-healing properties of vulcanized rubbers by replacing the conventional zinc oxide (ZnO) and stearic acid (SA) activator/coactivator system with ω-propenyl functional oligomers of poly(zinc methacrylate) (pZnMA), synthesized by catalytic chain transfer polymerization (CCTP). In addition to activating vulcanization, the pZnMA/ZnO complex allows the elastomers to be cured to a high degree while retaining their high self-healing efficiencies, as the ω-propenyl functional groups of the oligomers graft to the elastomer during vulcanization, reducing the number of permanent covalent cross-links as well as forming an ionic network throughout the compound. We then investigate the impact that adding carbon black has on the mechanical and self-healing properties of these vulcanized rubbers. Finally, the potential wet traction and rolling resistance properties of these rubbers are examined, which are important performance metrics for tire tread materials.[21,22]

EXPERIMENTAL SECTION

Materials. Natural rubber (NR, TSR10, Africa), stearic acid (SA), zinc oxide (ZnO), *N*-cyclohexyl-2-benzothiazolesulfenamide (CBS), and carbon black N234 (CB) were provided by Bridgestone EU NV/SA. Methacrylic acid (MAA) and zinc dimethacrylate (ZDMA) were purchased from Sigma-Aldrich. 2,2′-Azobis[2-(2-imidazolin-2-yl)-propane] dihydrochloride (VA-044) was obtained from Wako and used as received. Bis(boron difluorodimethylglyoximate)cobalt(II) methanol [$(CH_3OH)_2$Co-($dmgBF_2$) or (CoBF)] was synthesized by using a procedure described in the literature.[23]

Synthesis of ω-Propenyl Oligomers of Zinc Methacrylate (pZnMA/ZnO). Oligomers of pMAA were synthesized by catalytic chain transfer polymerization (CCTP, Figure 1a) following a procedure modified from our previous work.[24] Briefly, CoBF (46.17 mg, 120 ppm relative to final monomer concentration) was added to a 250 mL round-bottom flask (RBF) along with a magnetic stirrer and deoxygenated by nitrogen sparging for 1 h. MAA (90 mL) was added to a separate 250 mL RBF and also deoxygenated by nitrogen sparging for 1 h. The deoxygenated MAA (86 mL, 1 mol) was transferred to the CoBF by using a deoxygenated syringe. A small amount of deoxygenated methanol (∼10 mL) was added to the mixture to help fully dissolve the CoBF. VA-044 initiator (1.161 g, 5 mmol) and DI water (360 mL) were added to a 1 L three-necked round-bottom flask and were deoxygenated by nitrogen sparging for 1 h. The MAA/CoBF solution was then transferred into the initiator/solvent RBF with a deoxygenated syringe, and the mixture was heated to 55 °C with continuous stirring. The reaction was then continued for 5 h before being stopped by exposing it to air and allowing it to cool. The product was then freeze-dried for 48 h (Figure S1a). ^{1}H NMR (DMSO-d_6, 400 MHz) δ (ppm): 12.29 (s, −COO**H**), 6.08 (s, *cis* $\mathbf{H}_2$C=C−), 5.54 (d, *trans* $\mathbf{H}_2$C=C−), 1.5−4.0 (m, −C−C$\mathbf{H}_2$−C−), 0.5−1.5 (m, −C−C$\mathbf{H}_3$). Conversion (^{1}H NMR) = 96.52%, DP (^{1}H NMR) = 5, and M_n (^{1}H NMR) = 430 g/mol.

The dried pMAA (50 g, 116.28 mmol) was redissolved in deionized water, and then ZnO (50 g, 614.40 mmol) was added; the mixture was allowed to stir for 2 h at room temperature. The mixture was subsequently freeze-dried for 48 h to form a fine white powder of pZnMA/ZnO (Figure S1b).

Natural Rubber Vulcanization. Natural rubber (NR) compounds were prepared by using a Haake Polylab internal mixer at a rotor speed of 70 rpm and an initial temperature of 50 °C and then cured into 100 mm × 100 mm × 1 mm sheets at 150 °C under 20 MPa according to their t_{90} curing time measured by a moving die rheometer.

All of the samples contain (sulfur 0.7 (parts per hundred (phr), CBS 0.14 phr) with varied activator systems. Specifically, the control NR sample follows a conventional vulcanized formulation containing a curing activator (stearic acid/ZnO 1/5 phr, denoted as CV-ZS). By replacing the curing activator with pZnMA/ZnO (10, 15, and 20 phr), the resultant NR samples were denoted as CV-P1, CV-P2, and CV-P3, respectively. By replacing stearic acid/ZnO with ZDMA/ZnO (13.68/6.32 phr), the NR sample (CV-M) was obtained. The additional ZnO in CV-M was added to match the Zn content of CV-

https://doi.org/10.1021/acsapm.2c01398
ACS Appl. Polym. Mater. XXXX, XXX, XXX−XXX

P3. To evaluate the effect of carbon black, CV-P-CB1/2/3 samples were prepared by adding 10/25/40 phr of CB N234 to CV-P3. A table of these formulations is given in Table S1.

Analysis and Characterization. ^{1}H NMR spectra were recorded on a Bruker DPX-400 spectrometer in DMSO-d_6. Scanning electron microscopy (SEM) was conducted on a Zeiss SUPRA 55-VP scanning electron microscope with a field emission electron gun. An InLens detector was used at a working distance of 3.5 mm, an aperture size of 30 μm, and an acceleration voltage of 5 kV. Rubber samples were attached to aluminum specimen stubs with silver paint and then coated with carbon. A line of silver paint was then used to ground the rubber surface to the aluminum stub.

Tensile tests were on a Shimadzu Autograph AGS-X tester. Dumbbell specimens were cut according to ASTM-D638-14 type V. The tensile rate used was 100 mm/min with a 10 kN load cell, and the tests were performed at 19 °C. Cyclic stress softening tests were performed by elongating specimens to between 0% and 500% for five cycles at a tensile rate of 100 mm/min. A lap-shear test was conducted to evaluate the self-healing performance of the vulcanized NR, as illustrated in Figure S3. To ensure good contact, a force of 20 N was used, and self-healing was assessed at both room temperature and 80 °C. Dynamic mechanical thermal analysis (DMTA) was performed on samples approximately 6 mm × 10 mm × 2 mm in tension mode at a 1% strain and a frequency of 5 Hz, in the temperature range of −80 and 100 °C.

To measure the total cross-link density of rubbers, ∼0.5 g of each sample was first added to 100 mL of toluene and left for 7 days to reach equilibrium swelling. Swollen specimens were then weighed before being dried in a vacuum oven at 60 °C for 4 days. The weight of the dried samples was then recorded, and the cross-link densities (V_e) were calculated via eq 1.[16]

$$V_e = \frac{-[\ln(1-\Phi_r) + \Phi_r + \chi\Phi_r^2]}{V_0(\Phi_r^{1/3} - \Phi_r/2)} \quad (1)$$

where χ is the Flory−Huggins polymer−solvent interactions parameter (0.393),[25] V_0 is the molar volume of solvent (106.27), and Φ_r is the volume fraction, which was calculated via eq 2.

$$\Phi_r = \frac{m_2/\rho_2}{m_2/\rho_2 + (m_1 - m_2)/\rho_1} \quad (2)$$

where m_1 is the mass of the swollen samples, m_2 is the mass of the dried specimen, ρ_1 is the density of toluene (0.865 g/cm^3), and ρ_2 is the density of rubber. To measure the ionic cross-link densities, for the first 3 days specimens were swelled in a 90:10 mixture of toluene and formic acid before the solvent was switched to fresh toluene each day for 4 days. The cross-link density was then calculated as above and represented the remaining covalent cross-links. The ionic cross-link density was calculated by subtracting this value from the total cross-link density of each sample.

The strain-induced crystallization (SIC) of the rubber compounds CV-ZS and CV-P3 was observed from 2D small- and wide-angle X-ray scattering (SAXS/WAXS) measurements using a Xenocs Xeuss 2.0 X-ray instrument, operating with a wavelength λ = 1.54 Å. The rubber dumbbell samples were drawn by using a Linkam TST350 tensile testing stage which was positioned vertically in the X-ray instrument's evacuated sample chamber. The sample was positioned in the instrument jaws and cooled to a temperature of −30 °C and then drawn at a rate of 10 mm/min to a maximum extension of 700%. During the draw 2D SAXS/WAXS data were collected by using Pilatus 300K and Pilatus 100K detector systems, respectively. Both detectors were calibrated with silver behenate. Initially, full 2D WAXS was obtained from the Pilatus 300K detector positioned at a distance of 77.85 mm from the sample, and higher angle WAXS was obtained from the Pilatus 100K detector positioned at 162 mm from the sample. The 2D WAXS data were taken at a frame rate of 120 s. To obtain the 2D SAXS data, the Pilatus 300K detector was then positioned at a distance of 1.2 m from the sample. An evacuated chamber was positioned between the sample and the SAXS detector to reduce air scattering and absorption. The 2D SAXS data were taken at a frame rate of 120 s. All SAXS/WAXS data were normalized for sample thickness, transmission, and background scattering by using the Xeuss 2.0 instrument software. The 2D SAXS data were reduced to 1D scattering profiles of intensity (I) versus scattering vector q (where $q = (4\pi/\lambda)\sin(\theta)$, 2θ is the scattering angle and λ is the X-ray wavelength) by sector averaging around the beam stop by a fixed angle and radius, q.

RESULTS AND DISCUSSION

Synthesis of pZnMA/ZnO Activator by CCTP. Divalent metal oxides, such as Zn(II)O, have been used as a curing activator for rubber vulcanization for over 100 years.[26] Typically, stearic acid is also added as a coactivator, forming a zinc stearate complex that helps to ensure that there is a uniform dispersion of zinc throughout the rubber matrix. In this work, we have substituted the stearic acid component of this activator system with ω-propenyl functional oligomers of methacrylic acid (Figure 1), which complex with ZnO to form a pZnMA/ZnO salt. In this way, the complex acts as a vulcanization activator, while in addition a proportion of the vinyl groups of these oligomers couple to the NR backbone, forming an ionic network that enhances the self-healing properties of the final product.

Catalytic chain transfer polymerization (CCTP) is a radical polymerization technique that is ideal for the synthesis of low molecular weight ω-propenyl, α-protic oligomers of a range of vinyl monomers, most commonly methacrylates.[27] CCTP uses Co(II) complexes such as CoBF as chain transfer catalysts that abstract a β-hydrogen from a propagating radical chain, resulting in an oligomeric product and a Co(III)H complex that rapidly reinitiates the polymerization of a further monomer and returns to the Co(II) starting catalyst (Figure 1a). In this system, the molecular weight of the product is determined by the concentration ratio of catalyst to monomer, as described by the Mayo equation, where higher catalyst concentrations result in lower molecular weight products.[27] Because of the high activity of the Co(II) catalysts used in CCTP, the amounts required are in the parts per million (ppm) relative to monomer, which is ∼4 orders of magnitude higher than for the conventionally used thiols. This is one of the main reasons that this technique is highly scalable and useful for industrial applications. Recently, oligomers from CCTP have been used as reactive surfactants and emulsion stabilizers,[28−31] in pigment dispersants,[32] and as oil viscosity modifiers;[33] however, this is the first time they have been applied as additives to a rubber cure package.

To ensure that there were a high number of vinyl groups per unit weight added, and also to help dispersion in the rubber matrix, we aimed to prepare short oligomers of pMAA using a molar ratio of 120 ppm of CoBF relative to monomer. This is higher than would be typically required in the CCTP of methacrylates; however, the acidic conditions occurring in the polymerization of MAA can result in partial degradation of the catalyst, resulting in a lower chain transfer activity in these reactions.[34] Through integration of the ^{1}H NMR spectrum (Figure S2a), the DP of the pMAA oligomer was found to be ∼5 (M_n = 430 g/mol). In addition, from the DSC thermogram (Figure S2b), the T_g of the oligomers equaled 43.4 °C (onset, 55.9 °C endset). This is significantly lower than the literature T_g value for pMAA of 228 °C, as would be expected from the Flory−Fox equation for oligomers of this size. This low thermal transition temperature should improve the mobility of

https://doi.org/10.1021/acsapm.2c01398
ACS Appl. Polym. Mater. XXXX, XXX, XXX−XXX

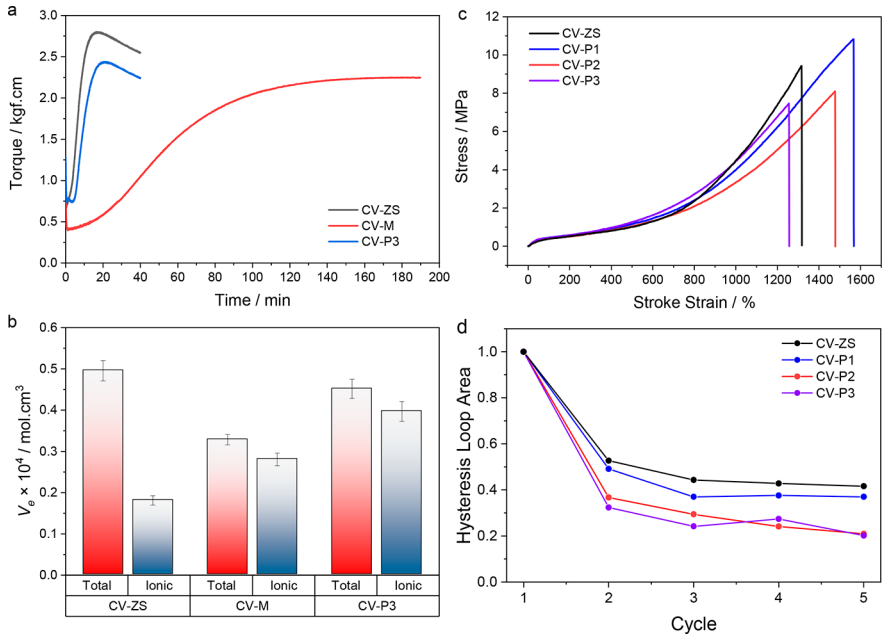

Figure 2. (a) Curing curves at 150 °C of CV-ZS, CV-M, and CV-P3. (b) Total and ionic cross-link densities of these samples determined by equilibrium swelling. (c) Typical stress−strain curves and (d) normalized hysteresis loop area during stress cycling of CV-ZS, CV-P1, CV-P2, and CV-P3.

these molecules within the rubber matrix during curing at 150 °C.

Mechanical Properties of Rubbers Vulcanized with pZnMA/ZnO Activator. To test the pZnMA/ZnO activator system, we selected a conventional accelerated curing system (CV) used in commercial natural rubber, where the weight ratio of sulfur to CBS accelerator is fixed at 5:1. The amount of sulfur and CBS relative to natural rubber was reduced to a quarter of a standard CV system, as this has been previously shown to facilitate some degree of self-healing due to a combination of reducing the cross-link density and increasing the ratio of disulfide to polysulfide cross-links in the network.[20] As mentioned above, it was found that the self-healing performance of these materials was enhanced by reducing their degree of curing to 50% (t_{50}); however, this came at the expense of reduced mechanical performance. Thus, to ensure optimal tensile properties, all samples in this work were cured to their t_{90}. To evaluate the effect of using pZnMA/ZnO as the activator, we also prepared compounds using the conventional stearic acid and ZnO (CV-ZS) as well as ZDMA and ZnO (CV-M) as activators. The curing curves of these samples are given in Figure 2a, and the curing times are given in Table S2.

It is apparent that pZnMA/ZnO activates curing with comparable efficiency to the ZnO/SA system, with t_{90} curing times of 11.1 and 14.75 min, respectively. In contrast, when the ZDMA/ZnO is used as the sole activator, the materials had poor curing properties, with a t_{90} curing time of 102.3 min. One contributing factor to the difference between the monomer and oligomer in these systems may be that the ω-propenyl-terminated oligomers are unable to homopolymerize,[35] and so the structures of their zinc complexes will be less affected by curing when compared with ZDMA, which could polymerize through the radicals generated during vulcanization.[36] This is interesting as ZDMA and zinc monomethacrylate (ZMMA) are sold under the brand names Sartomer SR708 and SR709, respectively, as commercial additives for accelerated sulfur vulcanization. However, they are typically used in conjunction with a stearic acid coactivator to provide efficient curing.[37]

The cross-link densities (V_e) of the vulcanized rubber products were determined by the equilibrium swelling method (Figure 2b). The total cross-link densities of the rubbers follow the same trend as the maximum torque values in their curing curves, confirming the differences in the number of cross-links formed when changing the activator system. To evaluate the number of ionic cross-links in these networks, we performed equilibrium swelling in a 90:10 mixture of toluene to formic acid for 3 days to break the ionic bonds, before exchanging the solvent for fresh toluene each day for 4 days to remove the residual formic acid. The samples cured with ZDMA/ZnO and pZnMA/ZnO show very high degrees of ionic cross-linking at 85.47 and 87.93% relative to the total, respectively. However, when using the same method with the CV-ZS control sample, an ionic cross-link density of 36.53% was recorded. It would be expected that the cross-links in CV-ZS should be only thioethers, disulfides, and polysulfides, and so some of these covalent bonds appear to be broken during the acid swelling, even when using a weak acid. Consequently, the ionic cross-link density in CV-M and CV-P3 is likely to be lower than was recorded here, but they are clearly higher in these samples than in the CV-ZS control, suggesting that an ionic network has been formed in these compounds.

When examining the effect that substituting stearic acid for ω-propenyl oligomers of MAA has on the mechanical properties of rubbers, we first added pMAA and ZnO separately to the rubber during compounding, as would be performed when using stearic acid. However, this resulted in a relatively low strength material, with a tensile strength of 3.96 ± 0.43 MPa (CV-P1*, Figure S4). This may be due to the pMAA partially agglomerating in the rubber matrix, which would result in weak aggregates distributed throughout the final material. In contrast, when adding these as a preformed salt of pZnMA/ZnO, the materials had a tensile strength of 10.83 ± 0.78 MPa and an elongation at break of 1568 ± 72%

https://doi.org/10.1021/acsapm.2c01398
ACS Appl. Polym. Mater. XXXX, XXX, XXX−XXX

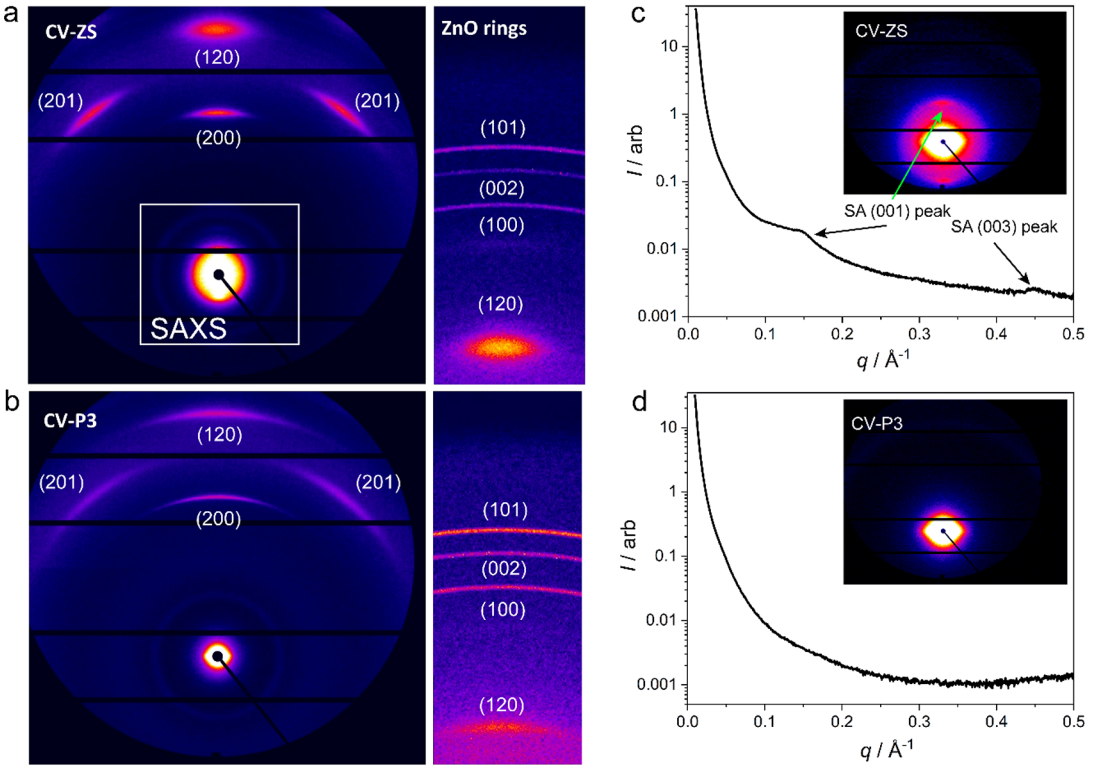

Figure 3. Oriented WAXS patterns of (a) CV-ZS and (b) CV-P3 under 700% elongation at −30 °C. Bragg peaks are indexed on the patterns. To the right of each pattern is an expansion of the WAXS pattern at high angles (2θ = 20°−45°), showing the ZnO crystalline Bragg rings. (c, d) 2D SAXS patterns and corresponding 1D profiles of CV-ZS and CV-P3, respectively, showing the presence and absence of stearic acid (SA) peaks at low angles. The draw direction is horizontal in all patterns.

(CV-P1, Figure S4). As shown in the typical stress−strain curves given in Figure 2c, this is slightly stronger than the CV-ZS control sample, which has a tensile strength of 8.61 ± 1.17 MPa and an elongation at break of 1277 ± 58%. The addition of more pZnMA/ZnO resulted in a slight reduction in mechanical properties, with measured tensile strengths of 8.09 ± 0.49 MPa for CV-P2 and 7.47 ± 0.64 MPa for CV-P3. This may be due to the increasing degree of substitution of sulfur cross-links for ionic bonds slightly weakening the material.

Cyclic stress−strain experiments were conducted on the modified rubbers CV-P1/2/3 as well as CV-ZS (Figure S5). As shown in Figure 2d, in all cases we observed a large decrease in the hysteresis loop area after the first cycle, due to the Mullin's effect.[38] However, the samples with pZnMA/ZnO displayed a larger degree of hysteresis. There is also some correlation between the amount of pZnMA/ZnO added and the decrease in the area of the hysteresis loop, with larger amounts generally exhibiting greater decreases. This is further evidence that when curing in the presence of pZnMA/ZnO the sulfur cross-links in CV-ZS are partially substituted by ionic associations, as these dynamic bonds should rupture more easily during stress cycling, resulting in larger energy dissipation.

An additional cause of hysteresis in vulcanized natural rubber is the energy required to alter its microstructure during strain-induced crystallization (SIC).[39] SIC is an important property in these materials, being the principal reason for their excellent mechanical properties and resistance to crack growth. To examine the SIC properties of the rubbers 2D small- and wide-angle X-ray scattering (SAXS/WAXS) patterns were obtained during the extension of samples to a maximum elongation of 700% at a temperature of −30 °C. The 2D WAXS patterns for CV-ZS and CV-P3 extended to 700% are given in Figures 3a and 3b, respectively. Both samples show that a highly oriented crystalline structure develops, evidenced by the Bragg peaks indexed as (120), (200), and (201),[40] with 2θ positions of 14.4°, 18.0°, and 21.3°, respectively. These can be assigned to the monoclinic unit cell where a = 12.5 Å, b = 8.9 Å, c = 8.1 Å, and β = 92°, as proposed by Bunn for natural rubber.[41] Figure S6 shows selected 2D WAXS data during the drawing of CV-ZS and CV-P3; here for CV-ZS, at an extension of ∼400%, the (120) and (200) peaks start to appear, indicating the onset of SIC. The peaks increase in intensity as the strain is increased to 700%, which has been observed previously in natural rubber systems.[42,43] Similarly, for CV-P3 the (200) peak, although weak in intensity, is observed at an extension of ∼400%, and the SIC develops on further extension. Hence, both samples show SIC readily occurs on elongation at low temperatures. The lower intensity observed in CV-P3 may indicate that pZnMA/ZnO impacts the SIC of this compound, resulting in its slightly lower mechanical strength; however, another contributing factor to this is the greater degree of structural rearrangement occurring in this sample that allows crystallized structures to relax during the measurement.

In the higher angle WAXS patterns, shown on the right of Figures 3a and 3b, Bragg rings indexed as (100), (002), and (101) with 2θ positions of 31.9°, 34.6°, and 36.4°, respectively, from the unoriented ZnO crystals can also be observed in both samples (note that the additional (120) peak from oriented rubber is labeled on both patterns). The greater intensity of the ZnO rings in the CV-P3 WAXS pattern is attributed to the higher concentration of ZnO in this formulation. Another

https://doi.org/10.1021/acsapm.2c01398
ACS Appl. Polym. Mater. XXXX, XXX, XXX−XXX

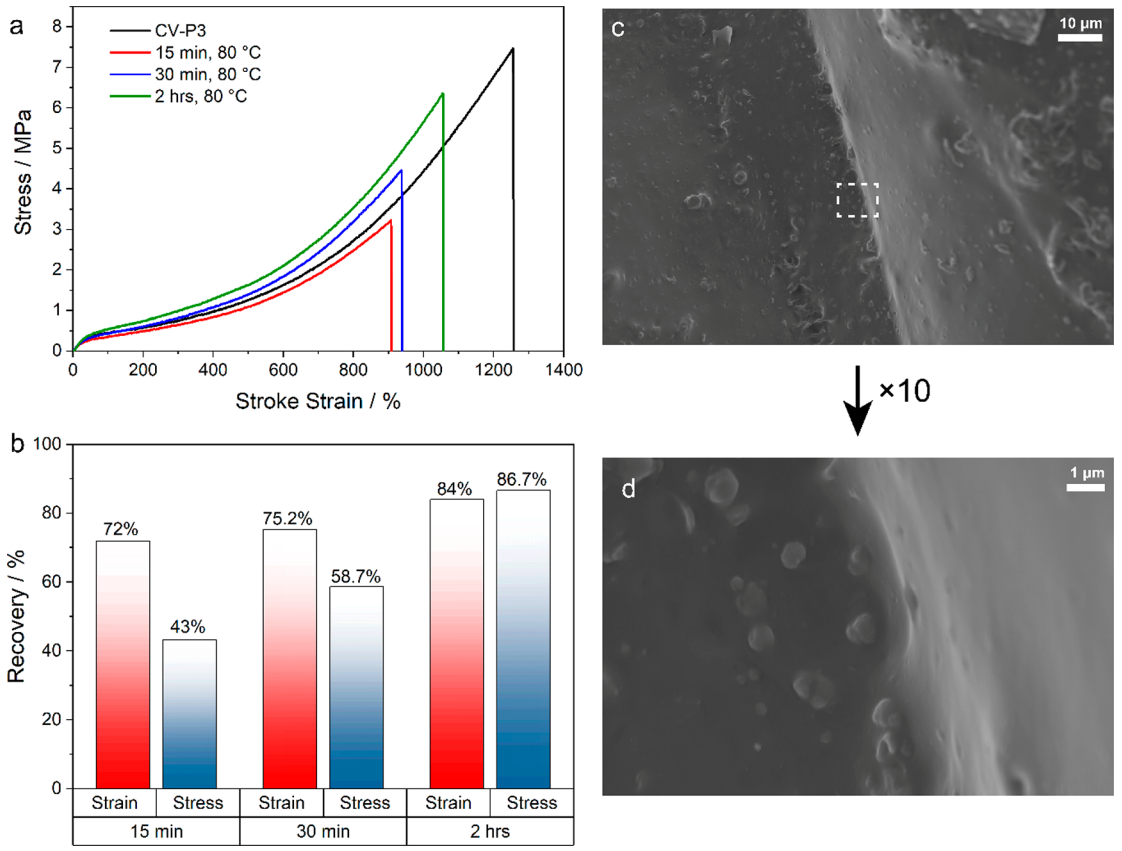

Figure 4. (a) Typical stress−strain curves of pristine CV-P3 as well as CV-P3 after being cut and self-healed for various times at 80 °C;(b) self-healing efficiencies of CV-P3; (c) SEM image of the self-healed area of CV-P3 after 2 h at 80 °C; and (d) a higher magnification in SEM image of the region highlighted in white in (c).

feature during the SIC of CV-ZS is observed in the SAXS patterns in Figures 3c and 3d, which is the expanded area labeled in Figure 3a. In Figure 3c, the 2D and corresponding 1D SAXS profiles show the stearic acid (SA) (001) and (003) peaks, which form as oriented crystalline platelets during the drawing process.[43,44] However, these peaks are absent from the CV-P3 trace, given in Figure 3d, as stearic acid was not used in this formulation.

Self-Healing Performance of Vulcanized Natural Rubbers. As previously mentioned, the CV system selected has been previously shown to produce materials with some self-healing ability, in particular when a low degree of curing is used.[20] In this work it was found that samples of CV-ZS that were cured to their t_{90} had good mechanical properties but were only able to recover 13.70% of their tensile strength and 29.76% of their elongation at break after being cut and allowed to self-heal at 80 °C for 30 min (Figure S7a). By contrast, CV-M had excellent self-healing performance, recovering 91.35% of its tensile strength and 81.22% of its elongation at break under the same conditions (Figure S7b). However, this material exhibited poor tensile properties, with a tensile strength of just 1.19 ± 0.22 MPa. These examples highlight the trade-off that often exists between the mechanical performance and self-healing ability of these materials.[45]

Using pZnMA/ZnO as the activator in these systems resulted in improved self-healing performance, as shown in Figures S8 and 4. In all cases it appears that the strain properties recover faster than mechanical strength in these materials; however, this is due to the nonlinear relationship between stress and strain in rubber compounds, as they become harder to deform at larger strains. The most promising compound we evaluated was CV-P3, which contained 20 phr of the pZnMA/ZnO. As shown in Figure 4, after just 15 min at 80 °C it recovered 43% of its tensile strength, and this increased to 58.7% after 30 min and 86.7% after 2 h. Considering that the tensile strength of CV-P3 is comparable to CV-ZS at 7.47 ± 0.64 MPa, this compound achieved an excellent balance between its mechanical and self-healing performance.

During tensile testing of the self-healed samples, they typically broke outside of the overlapped region, as illustrated on the right of Figure S3. This suggests that under the self-healing conditions a high degree of chain diffusion occurs at the interface between the two cut dumbbell pieces, which is facilitated by the exchange of bonds in the ionic network. To observe this more closely, SEM images were taken of this interface from specimens that had been self-healed for 2 h at 80 °C. Figure 4c shows the boundary between the self-healed surfaces, where one surface is slightly raised due to imperfect alignment when they were overlapped prior to being subjected to the self-healing conditions. However, it is apparent that there is good contact across this region. At a higher magnification, in Figure 4d, it appears that the surface between these two layers is continuous. This further demonstrates the high degree of chain diffusion that occurs during self-healing, resulting in the restoration of properties observed in Figure 4a.

For tire tread materials, carbon black or silica is often incorporated to improve mechanical performance, increase processing yield, and reduce costs. In particular, carbon black plays an important role due to its excellent reinforcing

https://doi.org/10.1021/acsapm.2c01398
ACS Appl. Polym. Mater. XXXX, XXX, XXX−XXX

properties.[46] Here we investigated the effect carbon black has on the mechanical properties and self-healing performance of CV-P3. Figure 5a shows typical stress−strain curves of CV-P3

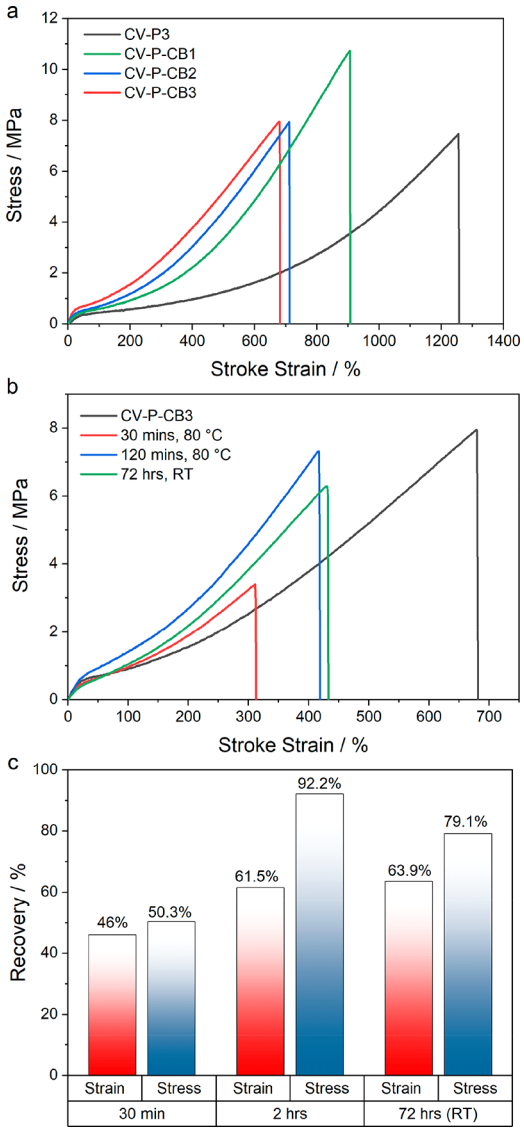

Figure 5. (a) Effect of carbon black loading on the mechanical properties of rubbers, (b) typical stress−strain curves of pristine CV-P-CB3 and samples that had been cut self-healed, and (c) self-healing efficiency of CV-P-CB3 after being held at 80 °C for 30 min and 2 h and at room temperature (RT) for 72 h.

samples containing carbon black N234 at 10, 25, and 40 phr, which are labeled CV-P-CB1, CV-P-CB2, and CV-P-CB3, respectively. Addition of 10 phr of carbon black results in an increase in tensile strength to 9.26 ± 1.32 MPa and a decrease in elongating at break to 872.25 ± 50%. Increasing the amount of carbon black to 25 phr resulted in a further decrease in the elongation at break to 690 ± 25%, along with a reduction in tensile strength to 7.28 ± 0.56 MPa. Further increase in loading to 40 phr resulted in little change, with CV-P-CB3 having a tensile strength of 7.56 ± 0.52 MPa and an elongation at break of 690 ± 9%. The reinforcement index (RI = $M_{300\%}/M_{100\%}$) of these rubbers shows the same trend as their tensile strength, with values of RI = 2.389, 2.795, and 2.783 for CV-P-CB1, CV-P-CB2, and CV-P-CB3, respectively. The RI gives an indication of the reinforcing effect of the filler at larger deformations and is positively correlated to the amount of bound rubber in the compound. As the RI did not increase when the amount of carbon black was increased from 25 to 40 phr, this suggests that there is a higher proportion of filler−filler interactions in CV-P-CB3 than are present in CV-P-CB2.

The self-healing properties of the composite samples are given in Figures 5b,c and S9. The recovery of CV-P-CB1 after self-healing at 80 °C for 2 h was slightly lower than that of CV-P3, with just a 55% recovery of the original tensile stress. However, as this composite has a higher tensile strength when compared to the unfilled rubber, this still translates into a material with a tensile strength of greater than 5 MPa after self-healing. Interestingly, for the CV-P-CB2 and CV-P-CV3, the recovery of tensile strength under these conditions increased to 90 and 93%, respectively. This shows that the complex range of chemical and physical interactions that occur in carbon black filled rubber can allow for and even enhance, the interdiffusion of chains and facilitate self-healing in these materials. However, all of the composite samples that were tested also had poorer recoveries of their tensile strains after self-healing at 80 °C compared with the unfilled CV-P3. This may be due to stress increasing more rapidly with strain in the composites.

A further interesting observation from the composites was the ability of CV-P-CV3 to self-heal at room temperature. Dumbbell specimens were cut and overlapped, as shown in Figure S3 and left for 72 h. From Figure 5, this resulted in a tensile strength recovery of 79.1%. The room temperature self-healing of the unfilled samples was also tested, as shown in Figure S8. Although in these examples it was clear that there was only weak surface adhesion holding them together, whereas CV-P-CB3 was much stronger and even broke outside of the overlapped region during tensile testing. The origin of these low-temperature self-healing properties may be that the carbon black acts as a solid lubricant that increases the mobility of the polymer chains. However, to date, there has been very little research into the effect of carbon black on the self-healing properties of vulcanized natural rubber. The only research paper that was found in the literature showed that self-healing efficiencies decreased with increasing carbon black content.[47] In this work, a dicumyl peroxide cured system was used, a different grade of carbon black (N330), as well as a different cross-linker (zinc thiolate), which could explain the different trends that were observed. Given the importance of carbon black within the tire industry, it is clear that this is an area where significantly more research is needed.

Dynamic Mechanical Analysis of Self-Healing Compounds. The rubbers developed in this current work were found to have an exceptional balance between their mechanical properties and self-healing efficiency. To evaluate their structural properties further, we used DMTA to evaluate the temperature dependence of the loss factor (tan δ). From Figure 6a, we see a small shift in the peak tan δ value with the addition of pZnMA/ZnO, which is at −53 °C for CV-ZS and shifts slightly to −50 °C for CV-P3. There is also a significant decrease in the magnitude of the peak tan δ value with the addition of 40 phr of carbon black, which is due to the reinforcing filler having a greater effect on the storage modulus (G', inset of Figure 6a) compared with the loss modulus (G'') around this region, as shown in Figure S10.[48]

The region between 0 and 60 °C of the tan δ versus temperature curve can be used as an indicator of key tire tread material performance metrics, such as wet traction and rolling

https://doi.org/10.1021/acsapm.2c01398
ACS Appl. Polym. Mater. XXXX, XXX, XXX−XXX

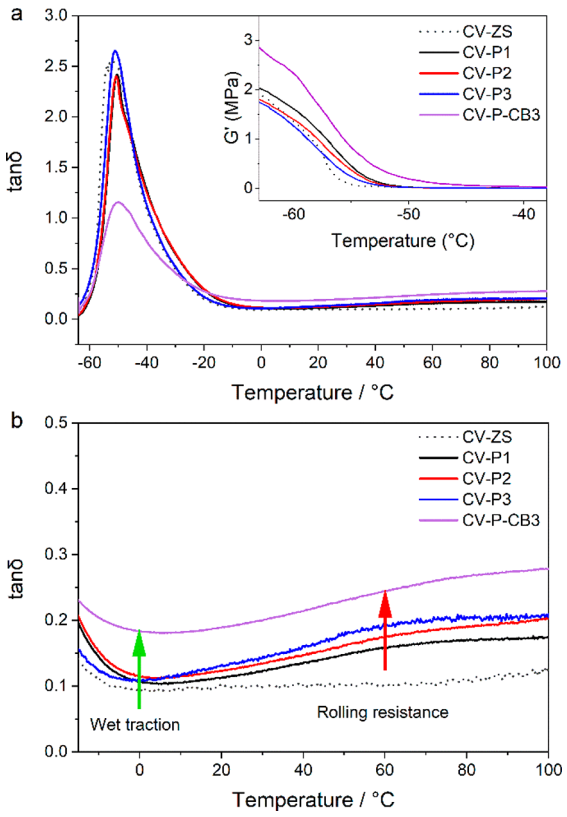

Figure 6. (a) Change in the tan δ with temperature as measured by DMTA. (b) Magnification between −15 and 100 °C highlighting the temperatures indicative of wet grip and rolling resistance.

resistance (or fuel efficiency).[49] From Figure 6b, it is apparent that with the addition of pZnMA/ZnO there is a small increase in wet traction, as indicated by the tan δ value at 0 °C. The addition of carbon black increases this further, as is typical for fine carbon blacks such as N234.[50] However, all samples with added pZnMA/ZnO showed significantly higher tan δ values at 60 °C, which suggests a higher rolling resistance than CV-ZS. These results indicate that fuel efficiency is an additional factor that needs to be balanced in self-healing compounds if they are to be used in tire tread materials.

CONCLUSIONS

In summary, ω-propenyl functional oligomers of pMAA were synthesized by CCTP and used to form a vulcanization activator complex, pZnMA/ZnO. The substitution of ZnO/SA for pZnMA/ZnO in a self-healing CV system resulted in materials with similar curing characteristics and total cross-link densities. However, a significant proportion of the cross-links in the compounds with pZnMA/ZnO were ionic bonds, which we postulate are formed between pZnMA units that were grafted to the NR backbone during vulcanization. The introduction of an ionic network only had a small effect on the tensile properties of the compounds, with the samples with 20 phr pZnMA/ZnO (CV-P3) having a tensile strength of 7.47 ± 0.64 MPa, compared with 8.61 ± 1.17 MPa for CV-ZS. However, the self-healing efficiency of samples with pZnMA/ZnO increased dramatically, with up to 86.7% recovery of tensile strength and 84% recovery of elongation at break after 2 h at 80 °C. This is compared with a 13.7% and 29.76% recovery of tensile strength and elongation at break, respectively, for CV-ZS.

Interestingly, it was found that the addition of carbon black N234 could simultaneously improve the mechanical properties of the rubber vulcanizates as well as increase their self-healing efficiency at 80 °C. At a carbon black loading of 40 phr, samples were also found to have excellent self-healing ability at room temperature, recovering 79.1% of their tensile strength after 72 h. This property could have a significant impact on the service life of these materials when used in tires. It was also found that both the pZnMA/ZnO curing additive and carbon black increased the tan δ at 0 °C, indicating that these composites would have improved wet traction performance. However, it is noted that more work needs to be done to improve the fuel efficiency of these materials and their overall life cycle effect on the environment.

ASSOCIATED CONTENT

Supporting Information

The Supporting Information is available free of charge at https://pubs.acs.org/doi/10.1021/acsapm.2c01398.

Experimental procedures, polymer characterization data, and data from our materials testing (PDF)

AUTHOR INFORMATION

Corresponding Author

Chaoying Wan − *International Institute for Nanocomposites Manufacturing (IINM), WMG, University of Warwick, Coventry CV4 7AL, U.K.*; orcid.org/0000-0002-1079-5885; Email: chaoying.wan@warwick.ac.uk

Authors

Alan M. Wemyss − *International Institute for Nanocomposites Manufacturing (IINM), WMG, University of Warwick, Coventry CV4 7AL, U.K.*; orcid.org/0000-0002-5919-9881

Arkadios Marathianos − *Department of Chemistry, University of Warwick, Coventry CV4 7AL, U.K.*

Ellen L. Heeley − *School of Life, Health and Chemical Sciences, The Open University, Milton Keynes MK7 6AA, U.K.*

James Ekeocha − *International Institute for Nanocomposites Manufacturing (IINM), WMG, University of Warwick, Coventry CV4 7AL, U.K.*

Yoshihiro Morishita − *Advanced Materials Division, Bridgestone Corporation, Tokyo 187-8531, Japan*

Raffaele di Ronza − *Bridgestone EU NV/SA, Italian Branch-Technical Center, 00128 Rome, Italy*

M. Mar Bernal − *Bridgestone EU NV/SA, Italian Branch-Technical Center, 00128 Rome, Italy*

David M. Haddleton − *Department of Chemistry, University of Warwick, Coventry CV4 7AL, U.K.*; orcid.org/0000-0002-4965-0827

Complete contact information is available at: https://pubs.acs.org/10.1021/acsapm.2c01398

Notes

The authors declare no competing financial interest.

ACKNOWLEDGMENTS

We gratefully acknowledge funding support from Bridgestone, the University of Warwick, and the WMG High Value Manufacturing Catapult Centre. The authors acknowledge the support from Dr. Steven Huband and the X-ray Diffraction

RTP (University of Warwick) for SAXS/WAXS data collection and processing and the Polymer Characterisation RTP (University of Warwick) part funded by EPSRC (EP/R511547/1).

REFERENCES

(1) Dong, Y.; Zhao, Y.; Hossain, M. U.; He, Y.; Liu, P. Life cycle assessment of vehicle tires: A systematic review. *Cleaner Environmental Systems* **2021**, *2*, 100033.
(2) Liu, L.; Cai, G.; Zhang, J.; Liu, X.; Liu, K. Evaluation of engineering properties and environmental effect of recycled waste tire-sand/soil in geotechnical engineering: A compressive review. *Renewable and Sustainable Energy Reviews* **2020**, *126*, 109831.
(3) Wemyss, A. M.; Bowen, C.; Plesse, C.; Vancaeyzeele, C.; Nguyen, G. T. M.; Vidal, F.; Wan, C. Dynamic crosslinked rubbers for a green future: A material perspective. *Materials Science and Engineering: R: Reports* **2020**, *141*, 100561.
(4) Abdul-Kader, W.; Haque, M. S. Sustainable tyre remanufacturing: an agent-based simulation modelling approach. *International Journal of Sustainable Engineering* **2011**, *4* (4), 330−347.
(5) Wemyss, A. M.; Ellingford, C.; Morishita, Y.; Bowen, C.; Wan, C. Dynamic Polymer Networks: A New Avenue towards Sustainable and Advanced Soft Machines. *Angew. Chem., Int. Ed.* **2021**, *60* (25), 13725−13736.
(6) Ekeocha, J.; Ellingford, C.; Pan, M.; Wemyss, A. M.; Bowen, C.; Wan, C. Challenges and Opportunities of Self-Healing Polymers and Devices for Extreme and Hostile Environments. *Adv. Mater.* **2021**, *33*, 2008052.
(7) Wang, S.; Urban, M. W. Self-healing polymers. *Nat. Rev. Mater.* **2020**, *5* (8), 562−583.
(8) Tanasi, P.; Hernández Santana, M.; Carretero-González, J.; Verdejo, R.; López-Manchado, M. A. Thermoreversible crosslinked natural rubber: A Diels-Alder route for reuse and self-healing properties in elastomers. *Polymer* **2019**, *175*, 15−24.
(9) Jia, Z.; Zhu, S.; Chen, Y.; Zhang, W.; Zhong, B.; Jia, D. Recyclable and self-healing rubber composites based on thermoreversible dynamic covalent bonding. *Composites Part A: Applied Science and Manufacturing* **2020**, *129*, 105709.
(10) Cheng, B.; Lu, X.; Zhou, J.; Qin, R.; Yang, Y. Dual Cross-Linked Self-Healing and Recyclable Epoxidized Natural Rubber Based on Multiple Reversible Effects. *ACS Sustainable Chem. Eng.* **2019**, *7* (4), 4443−4455.
(11) Imbernon, L.; Oikonomou, E. K.; Norvez, S.; Leibler, L. Chemically crosslinked yet reprocessable epoxidized natural rubber via thermo-activated disulfide rearrangements. *Polym. Chem.* **2015**, *6* (23), 4271−4278.
(12) Bapat, A. P.; Sumerlin, B. S.; Sutti, A. Bulk network polymers with dynamic B−O bonds: healable and reprocessable materials. *Materials Horizons* **2020**, *7* (3), 694−714.
(13) Chen, Y.; Tang, Z.; Zhang, X.; Liu, Y.; Wu, S.; Guo, B. Covalently Cross-Linked Elastomers with Self-Healing and Malleable Abilities Enabled by Boronic Ester Bonds. *ACS Appl. Mater. Interfaces* **2018**, *10* (28), 24224−24231.
(14) Liu, Y.; Li, Z.; Liu, R.; Liang, Z.; Yang, J.; Zhang, R.; Zhou, Z.; Nie, Y. Design of Self-Healing Rubber by Introducing Ionic Interaction To Construct a Network Composed of Ionic and Covalent Cross-Linking. *Ind. Eng. Chem. Res.* **2019**, *58* (32), 14848−14858.
(15) Xu, C.; Cao, L.; Huang, X.; Chen, Y.; Lin, B.; Fu, L. Self-Healing Natural Rubber with Tailorable Mechanical Properties Based on Ionic Supramolecular Hybrid Network. *ACS Appl. Mater. Interfaces* **2017**, *9* (34), 29363−29373.
(16) Liu, J.; Xiao, C.; Tang, J.; Liu, Y.; Hua, J. Construction of a Dual Ionic Network in Natural Rubber with High Self-Healing Efficiency through Anionic Mechanism. *Ind. Eng. Chem. Res.* **2020**, *59* (28), 12755−12765.
(17) Xiang, H. P.; Qian, H. J.; Lu, Z. Y.; Rong, M. Z.; Zhang, M. Q. Crack healing and reclaiming of vulcanized rubber by triggering the rearrangement of inherent sulfur crosslinked networks. *Green Chem.* **2015**, *17* (8), 4315−4325.
(18) Xu, W.-Z.; Yu, W.-W.; Chen, X.; Liao, S.; Luo, M.-C. Based on transalkylation reaction the rearrangeable conventional sulfur network facile design for vulcanized diolefin elastomers. *J. Appl. Polym. Sci.* **2021**, *138* (40), 51182.
(19) Hernández, M.; Grande, A. M.; van der Zwaag, S.; García, S. J. Monitoring Network and Interfacial Healing Processes by Broadband Dielectric Spectroscopy: A Case Study on Natural Rubber. *ACS Appl. Mater. Interfaces* **2016**, *8* (16), 10647−10656.
(20) Hernández, M.; Grande, A. M.; Dierkes, W.; Bijleveld, J.; van der Zwaag, S.; García, S. J. Turning Vulcanized Natural Rubber into a Self-Healing Polymer: Effect of the Disulfide/Polysulfide Ratio. *ACS Sustainable Chem. Eng.* **2016**, *4* (10), 5776−5784.
(21) Araujo-Morera, J.; Hernández Santana, M.; Verdejo, R.; López-Manchado, M. A. Giving a Second Opportunity to Tire Waste: An Alternative Path for the Development of Sustainable Self-Healing Styrene−Butadiene Rubber Compounds Overcoming the Magic Triangle of Tires. *Polymers* **2019**, *11* (12), 2122.
(22) Utrera-Barrios, S.; Araujo-Morera, J.; Pulido de Los Reyes, L.; Verdugo Manzanares, R.; Verdejo, R.; López-Manchado, M. Á.; Hernández Santana, M. An effective and sustainable approach for achieving self-healing in nitrile rubber. *Eur. Polym. J.* **2020**, *139*, 110032.
(23) Zhang, Q.; Slavin, S.; Jones, M. W.; Haddleton, A. J.; Haddleton, D. M. Terminal functional glycopolymers via a combination of catalytic chain transfer polymerisation (CCTP) followed by three consecutive click reactions. *Polym. Chem.* **2012**, *3* (4), 1016−1023.
(24) Marathianos, A.; Wemyss, A. M.; Liarou, E.; Jones, J. R.; Shegiwal, A.; Town, J. S.; Lester, D. W.; Li, Y.; Haddleton, D. M. Controlling the Particle Size in Surfactant-Free Latexes from ω-Propenyl Oligomers Obtained through Catalytic Chain Transfer Polymerization. *ACS Appl. Polym. Mater.* **2021**, *3* (6), 3185−3196.
(25) Valentín, J. L.; Carretero-González, J.; Mora-Barrantes, I.; Chassé, W.; Saalwächter, K. Uncertainties in the Determination of Cross-Link Density by Equilibrium Swelling Experiments in Natural Rubber. *Macromolecules* **2008**, *41* (13), 4717−4729.
(26) Coran, A. Y. Chemistry of the vulcanization and protection of elastomers: A review of the achievements. *J. Appl. Polym. Sci.* **2003**, *87* (1), 24−30.
(27) Heuts, J. P. A.; Smeets, N. M. B. Catalytic chain transfer and its derived macromonomers. *Polym. Chem.* **2011**, *2* (11), 2407−2423.
(28) Shegiwal, A.; Wemyss, A. M.; Schellekens, M. A. J.; de Bont, J.; Town, J.; Liarou, E.; Patias, G.; Atkins, C. J.; Haddleton, D. M. Exploiting catalytic chain transfer polymerization for the synthesis of carboxylated latexes via sulfur-free RAFT. *J. Polym. Sci., Part A: Polym. Chem.* **2019**, *57* (3), E1−E9.
(29) Shegiwal, A.; Wemyss, A. M.; Liarou, E.; Town, J.; Patias, G.; Atkins, C. J.; Marathianos, A.; Lester, D. W.; Efstathiou, S.; Haddleton, D. M. Polymerisable surfactants for polymethacrylates using catalytic chain transfer polymerisation (CCTP) combined with sulfur free-RAFT in emulsion polymerisation. *Eur. Polym. J.* **2020**, *125*, 109491.
(30) Schreur-Piet, I.; Heuts, J. P. A. In situ stabilizer formation from methacrylic acid macromonomers in emulsion polymerization. *Polym. Chem.* **2017**, *8* (43), 6654−6664.
(31) Schreur-Piet, I.; Heuts, J. P. A. Amphiphilic Statistical Copolymers from Catalytic Chain Transfer as Reactive Surfactants in Emulsion Polymerization. *ACS Appl. Polym. Mater.* **2021**, *3*, 4616.
(32) Atkins, C. J.; Patias, G.; Town, J. S.; Wemyss, A. M.; Eissa, A. M.; Shegiwal, A.; Haddleton, D. M. A simple and versatile route to amphiphilic polymethacrylates: catalytic chain transfer polymerisation (CCTP) coupled with post-polymerisation modifications. *Polym. Chem.* **2019**, *10* (5), 646−655.
(33) Patias, G.; Wemyss, A. M.; Efstathiou, S.; Town, J. S.; Atkins, C. J.; Shegiwal, A.; Whitfield, R.; Haddleton, D. M. Controlled synthesis of methacrylate and acrylate diblock copolymers via end-capping using CCTP and FRP. *Polym. Chem.* **2019**, *10* (47), 6447−6455.

https://doi.org/10.1021/acsapm.2c01398
ACS Appl. Polym. Mater. XXXX, XXX, XXX−XXX

(34) Haddleton, D. M.; Depaquis, E.; Kelly, E. J.; Kukulj, D.; Morsley, S. R.; Bon, S. A. F.; Eason, M. D.; Steward, A. G. Cobalt-mediated catalytic chain-transfer polymerization (CCTP) in water and water/alcohol solution. *J. Polym. Sci., Part A: Polym. Chem.* **2001**, *39* (14), 2378−2384.
(35) Yamada, B.; Oku, F.; Harada, T. Substituted propenyl end groups as reactive intermediates in radical polymerization. *J. Polym. Sci., Part A: Polym. Chem.* **2003**, *41* (5), 645−654.
(36) Akiba, M.; Hashim, A. S. Vulcanization and crosslinking in elastomers. *Prog. Polym. Sci.* **1997**, *22* (3), 475−521.
(37) Monsallier, J.-M. Activate Accelerated Sulfur Vulcanization and Reduce Zinc Loading: Using Zinc Monomethacrylate. *Kautschuk, Gummi, Kunststoffe* **2009**, *62* (11), 597−604.
(38) Diani, J.; Fayolle, B.; Gilormini, P. A review on the Mullins effect. *Eur. Polym. J.* **2009**, *45* (3), 601−612.
(39) Le Cam, J. B. Energy storage due to strain-induced crystallization in natural rubber: The physical origin of the mechanical hysteresis. *Polymer* **2017**, *127*, 166−173.
(40) Chen, P.; Zhao, J.; Lin, Y.; Chang, J.; Meng, L.; Wang, D.; Chen, W.; Chen, L.; Li, L. In situ characterization of strain-induced crystallization of natural rubber by synchrotron radiation wide-angle X-ray diffraction: construction of a crystal network at low temperatures. *Soft Matter* **2019**, *15* (4), 734−743.
(41) Bunn, C. W.; Bragg, W. H. Molecular structure and rubber-like elasticity I. The crystal structures of β gutta-percha, rubber and polychloroprene. *Proc. R. Soc. London. Series A. Mathematical and Physical Sciences* **1942**, *180* (980), 40−66.
(42) Toki, S.; Sics, I.; Ran, S.; Liu, L.; Hsiao, B. S.; Murakami, S.; Senoo, K.; Kohjiya, S. New Insights into Structural Development in Natural Rubber during Uniaxial Deformation by In Situ Synchrotron X-ray Diffraction. *Macromolecules* **2002**, *35* (17), 6578−6584.
(43) Tosaka, M.; Murakami, S.; Poompradub, S.; Kohjiya, S.; Ikeda, Y.; Toki, S.; Sics, I.; Hsiao, B. S. Orientation and Crystallization of Natural Rubber Network As Revealed by WAXD Using Synchrotron Radiation. *Macromolecules* **2004**, *37* (9), 3299−3309.
(44) Liu, H.; Huang, G.-S.; Wei, L.-Y.; Zeng, J.; Fu, X.; Huang, C.; Wu, J.-R. Inhomogeneous Natural Network Promoting Strain-induced Crystallization: A Mesoscale Model of Natural Rubber. *Chin. J. Polym. Sci.* **2019**, *37* (11), 1142−1151.
(45) Efstathiou, S.; Wemyss, A. M.; Patias, G.; Al-Shok, L.; Grypioti, M.; Coursari, D.; Ma, C.; Atkins, C. J.; Shegiwal, A.; Wan, C.; Haddleton, D. M. Self-healing and mechanical performance of dynamic glycol chitosan hydrogel nanocomposites. *J. Mater. Chem. B* **2021**, *9* (3), 809−823.
(46) Jiang, X.; Zhang, L.; Wang, F.; Liu, Y.; Guo, Q.; Wang, C. Investigation of Carbon Black Production from Coal Tar via Chemical Looping Pyrolysis. *Energy Fuels* **2016**, *30* (4), 3535−3540.
(47) Khimi, S. R.; Syamsinar, S. N.; Najwa, T. N. L. Effect of Carbon Black on Self-healing Efficiency of Natural Rubber. *Materials Today: Proceedings* **2019**, *17*, 1064−1071.
(48) Robertson, C. G.; Lin, C. J.; Rackaitis, M.; Roland, C. M. Influence of Particle Size and Polymer−Filler Coupling on Viscoelastic Glass Transition of Particle-Reinforced Polymers. *Macromolecules* **2008**, *41* (7), 2727−2731.
(49) Araujo-Morera, J.; Hernández Santana, M.; Verdejo, R.; López-Manchado, M. A. Giving a Second Opportunity to Tire Waste: An Alternative Path for the Development of Sustainable Self-Healing Styrene−Butadiene Rubber Compounds Overcoming the Magic Triangle of Tires. *Polymers* **2019**, *11* (12), 2122.
(50) Hess, W. M.; Klamp, W. K. The Effects of Carbon Black and Other Compounding Variables on Tire Rolling Resistance and Traction. *Rubber Chem. Technol.* **1983**, *56* (2), 390−417.

https://doi.org/10.1021/acsapm.2c01398
ACS Appl. Polym. Mater. XXXX, XXX, XXX−XXX